

# **$\mathcal{J}$ FIT: a framework to obtain combined experimental results through joint fits**

E. Ben-Haim<sup>1</sup>, R. Brun<sup>2</sup>, B. Echenard<sup>3</sup>, T.E. Latham<sup>4</sup>

<sup>1</sup>*Laboratoire de Physique Nucléaire et de Hautes Energies (LPNHE),  
IN2P3/CNRS, Université Pierre et Marie Curie-Paris 6, Université Denis  
Diderot-Paris7*

<sup>2</sup>*European Organization for Nuclear Research (CERN), Geneva, Switzerland*

<sup>3</sup>*California Institute of Technology, Pasadena, California 91125, USA*

<sup>4</sup>*Department of Physics, University of Warwick, Coventry CV4 7AL, United  
Kingdom*

## **Abstract**

A framework is presented for obtaining combined experimental results through joint fits of datasets from several experiments. The  $\mathcal{J}$ FIT framework allows such fits to be performed keeping the data separated, in its original format, and using independent fitting environments, thus simplifying the process with respect to data access policies. It is based on a master-server architecture, using the network communication classes from ROOT. The framework provides an optimal way to exploit data from several experiments: it ensures that correlations are correctly taken into account and results in a better determination of nuisance parameters. Its advantages are discussed and illustrated by two examples from the domain of high energy physics.

## **1 Introduction**

Combining results of different experiments is a task that is routinely performed in high-energy physics. For this purpose, measured observables are usually assumed to be normally distributed and standard statistical prescriptions are readily applied. However, there are situations in which, even with the simple normal-distribution hypothesis, these methods are challenging to apply, such as for measurements involving a large number of parameters (including nuisance parameters). The size of the covariance matrices, when available, makes the procedure tedious and prone to errors. When non-Gaussian uncertainties are taken into account the combination procedure becomes much more complicated, as the complete likelihood functions are generally needed. This is indispensable in many complex measurements, in cases with small sample sizes and combination of upper limits. A dedicated tool for combining results would thus be desirable.

In the vast majority of cases, the parameters of interest are estimated by each experiment using a fit to their data. Ideally, combining such measurements would be equivalent to fitting simultaneously the different data samples. The straightforward solution involves collecting data in a common format, and has been implemented among others in the ROOFIT package [2]. This solution could however be inefficient

if dedicated fitting frameworks have already been developed. It may also raise issues with data access policies of each experiment. An alternative approach consists of performing a joint fit while keeping the data separated. This is easily achieved using a master-worker architecture, in which the master drives the fit by combining the values of the likelihood functions returned by several workers, each of which is specific to an experiment and accesses its own dataset. This solution presents several advantages:

- the data do not need to be rewritten in any external format, and can be readily used;
- collaborations can avoid sharing their data and procedures;
- any fitting algorithm can be readily incorporated in this scheme;
- all correlations are transparently taken into account;
- correlated and uncorrelated systematic uncertainties are easily included;
- common nuisance parameters are also determined jointly, allowing further improvement in precision.

In this paper we present **JFIT**: an implementation of this idea within the ROOT framework [3]. In section 2, we briefly review the maximum-likelihood technique and detail the **JFIT** joint fitting method in section 3. Two examples are given in section 4: a measurement of properties of a resonance, and an amplitude analysis of charmless  $B$ -mesons decays with a three-body final state.

## 2 Maximum-likelihood estimation

Maximum-likelihood estimation is a widely-used method of fitting parameters of a model to some data and providing an estimate of their uncertainties. In this section we briefly review this technique; more details can be found in statistics textbooks, and, for example, in Ref. [1].

Consider a set of  $N$  independent observations  $x_1, \dots, x_N$  of a random variable  $x$  following a probability density function (PDF) modelled by  $\mathcal{P}(x, \theta)$ , where  $\theta$  denotes the unknown model parameter(s) that should be estimated. Both  $x$  and  $\theta$  can be multidimensional. The likelihood function  $\mathcal{L}$  is defined as:

$$\mathcal{L}(\theta) = \prod_{i=1}^N \mathcal{P}(x_i, \theta). \quad (1)$$

Since the  $N$  observations  $x_i$  are given, the likelihood is only a function of  $\theta$ . The resulting estimate  $\hat{\theta}$  of the parameter  $\theta$  is defined as the value that maximises the likelihood, i.e.

$$\hat{\theta} = \max_{\theta} \mathcal{L}(\theta). \quad (2)$$

It is often convenient to minimise the negative logarithm of the likelihood (NLL) instead of maximising the likelihood. As the logarithmic function is monotonic,

both maximum-likelihood estimates yield the same value of  $\hat{\theta}$ . If the number of observations is random, an additional term is usually included in the likelihood to form the so-called extended likelihood:

$$\mathcal{L}_{\text{ext}}(\theta) = \frac{e^{-n} n^N}{N!} \prod_{i=1}^N \mathcal{P}(x_i, \theta), \quad (3)$$

where  $n$  denotes the expected number of events.

The formalism allowing the combination of different datasets (e.g., from different experiments) is well known: the total likelihood is simply given by the product of likelihoods from the different datasets. In the case of two datasets  $A$  and  $B$  (the generalisation to a larger number of datasets is straightforward), the combined likelihood is written as:

$$\mathcal{L}(\theta, \theta_A, \theta_B) = \prod_{x \in x_A} \mathcal{L}_A(\theta, \theta_A) \prod_{x \in x_B} \mathcal{L}_B(\theta, \theta_B), \quad (4)$$

where  $\theta$  denotes the parameters to extract from both datasets simultaneously, and  $\theta_A$  and  $\theta_B$  are those that are specific for  $A$  and  $B$ , respectively.

The minimisation of the NLL can be, and usually is, done numerically. Among the packages available to perform this task, MINUIT [4] is one of the most popular in the field of high energy physics. Its default algorithm, MIGRAD, is based on a variable-metric method that computes the value of the function and its gradient at each step of the procedure. If the functional form of the derivative is not, or cannot be supplied by the user, the gradient is evaluated by finite differences. The minimisation stops when the difference of the value of the function between two successive steps reaches a specific threshold. Parabolic uncertainties on the parameters are estimated by inverting the matrix of second derivatives evaluated at the minimum of the function. In the case of non-Gaussian likelihood, the uncertainties are estimated by an algorithm that scans the likelihood for each parameter separately, minimising the likelihood each time with respect to the remaining parameters.

### 3 Joint fits and the $\mathbf{J}_{\text{FIT}}$ method

In the following, we specifically consider the situation where several datasets have to be fitted jointly. The model to be fitted contains parameters that are shared by all datasets, such as  $\theta$  in Eq. 4 (common parameters), as well as parameters specific to each dataset, such as  $\theta_A$  and  $\theta_B$  in Eq. 4 (specific parameters). A simple example would be a one-dimensional fit to extract a parameter of interest, such as the mass of a resonance, from two datasets in which the signal and background distributions are modelled differently. As mentioned in the introduction, an approach based on a master-worker architecture,  $\mathbf{J}_{\text{FIT}}$ , can be used to perform such a fit. The master drives the fit by sending sets of parameters to the experiment-specific workers. Each worker returns the result of the function to minimise to the master, which updates the value of the parameters. The procedure is repeated until the fit has converged.

More precisely, this approach consists of the following steps:

- Initialisation: the master initialises the fit algorithm, e.g. MINUIT, including all parameters of the model, both common and specific to each worker (an alternative is discussed below). Each worker initialises its internal structure.
- Synchronisation: the master establishes a connection with each worker. In ROOT, this is done using the TMessage class<sup>1</sup>. The connections can be secured using ssh, for example.
- Minimisation: the master then sends the initial parameters to the workers. Each worker computes the value of the function to minimise and returns it to the master. The latter combines the results and updates the parameters accordingly. This step is repeated until convergence is achieved. The uncertainties on the parameters are evaluated by a similar procedure.
- Termination: the connections between the master and the workers are closed.

The overhead introduced by this procedure is small. For instance, in the example from Sec. 4.2 the time for each individual fit to be performed was  $33 \pm 6$  seconds, while the joint fits using the **JFIT** framework took  $35 \pm 5$  seconds.

An alternative scheme for handling nuisance parameters consists of fitting only the common parameters in the master process and declaring each set of specific parameters within the corresponding worker. At each step of the minimisation (i.e. each time the master sends a set of parameters), the workers perform an additional minimisation, keeping the common parameters fixed and minimising with respect to their specific parameters. The values of the minimised functions are then returned to the master.

Both procedures allow to reuse most of the code developed by each experiment for fitting their own data. They are both implemented in the Laura++ package [5].

Another advantage of performing a **JFIT** to combine results from two experiments is related to the estimation of systematic uncertainties and the correlations between them. Systematic uncertainties related to the common fit parameters are taken care of in the level of the master. These could originate, for instance, from fixing some of the physics parameters. Other systematic uncertainties, in the level of the parameters managed by the workers (e.g., fixed PDF-shape parameters), must be modified jointly by the two experiments before running a fit. Systematic uncertainties originating from external sources, such as those related to a measured branching fraction of a background, must be taken into account in a coherent way between the two experiments. These are usually considered as fully correlated in a naïve combination of results, while in reality different patterns of migration between event species in the two experiments may alter this behaviour. This is illustrated in the Sec. 4.1.

---

<sup>1</sup>This implementation is based on the ROOT macros:

<http://root.cern.ch/root/html/tutorials/net/authserv.C.html>

<http://root.cern.ch/root/html/tutorials/net/authclient.C.html>

## 4 Examples

### 4.1 Resonance mass and branching-fraction measurement

As a first example, we examine the problem of combining the results of two experiments that found a resonance in an invariant mass spectrum, at a mass of  $126 \text{ GeV}/c^2$ . The parameters of interest, the mass of the resonance,  $m_{\text{Res}}$ , and its branching fraction, BF, to the observed final state, are obtained from a one-dimensional maximum-likelihood fit to the distribution of invariant mass,  $m$ , of the final-state particles.

Samples corresponding to the datasets of experiments 1 and 2 are generated in the invariant-mass range of  $[100, 160] \text{ GeV}/c^2$  according to a model containing three events species: signal, peaking background and combinatorial background. Signal events are generated from a sum of two Crystal Ball (CB) functions [6]: core and tail, with different peak positions. Peaking and combinatorial background events are generated from a Gaussian and a fourth order Chebyshev polynomial function, respectively. This model is roughly inspired by the search of the Standard Model Higgs boson from ATLAS [7] and CMS [8], although, with rather different event yields and signal to background ratios. As the underlying physics is assumed to be unique, the same model is used to generate events for both experiments. To emulate in a simple way different overall efficiencies and event-selection strategies, the datasets corresponding to the two experiments have significantly different numbers of signal and background events. Five hundred pairs of datasets are generated, where the numbers of events of each species are Poisson-distributed, using PDFs that are summarised in Tab. 1. The invariant mass distribution of experiment 1 is shown in Fig. 1.

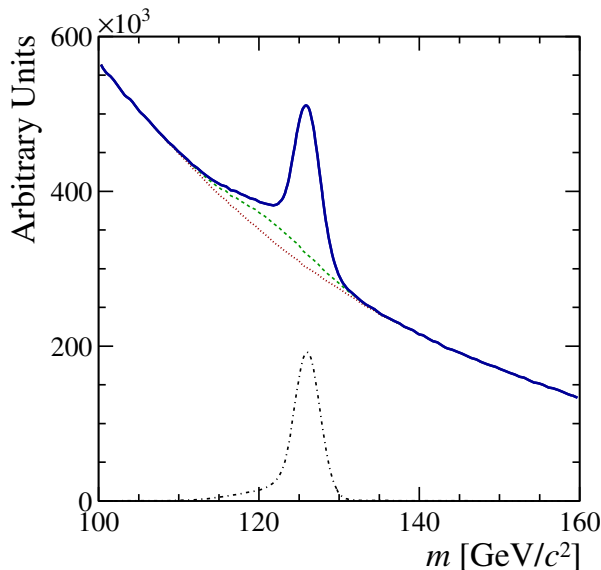


Figure 1: The invariant-mass distribution of a sample generated for experiment 1. The solid (blue) curve shows the full sample. The dash-dotted (black) curve corresponds to the distribution of signal events, while the dotted (red) and the dashed (green) curves show the distributions for the combinatorial and total background, respectively.

Table 1: Summary of the model used to generate events. The average number of events of each species generated per experiment is denoted  $N$ . The peak positions and Gaussian widths of the CB and Gaussian functions are denoted  $\mu$  and  $\sigma$ , respectively, with the superscript core or tail, and with the subscript CB, as appropriate. The CB tail parameters are  $\alpha$  and  $n$ . The coefficient of the  $i^{\text{th}}$  power term in the polynomial is denoted  $c_i$ .

Event species	Function	Parameter	Value
Signal	Sum of two CB functions (core and tail)	$N$ (experiment 1)	3000
		$N$ (experiment 2)	10000
		$\mu_{\text{CB}}^{\text{core}}$	126 GeV/ $c^2$
		$\sigma_{\text{CB}}^{\text{core}}$	1.6 GeV/ $c^2$
		$\alpha^{\text{core}}$	1.5
		$n^{\text{core}}$	3.0
		Fraction of tail	10%
		$\mu_{\text{CB}}^{\text{tail}}$	120 GeV/ $c^2$
		$\sigma_{\text{CB}}^{\text{tail}}$	4.0 GeV/ $c^2$
		$\alpha^{\text{tail}}$	-1.0
		$n^{\text{tail}}$	4.0
Peaking background	Gaussian	$N$ (experiment 1)	1000
		$N$ (experiment 2)	7500
		$\mu$	122 GeV/ $c^2$
		$\sigma$	5.0 GeV/ $c^2$
Combinatorial background	4 <sup>th</sup> order Chebyshev polynomial	$N$ (experiment 1)	60000
		$N$ (experiment 2)	500000
		$c_1$	-0.682
		$c_2$	0.122 [GeV/ $c^2$ ] <sup>-1</sup>
		$c_3$	-0.013 [GeV/ $c^2$ ] <sup>-2</sup>
		$c_4$	-0.003 [GeV/ $c^2$ ] <sup>-3</sup>

The maximum-likelihood fits are performed in the same  $[100, 160]$   $\text{GeV}/c^2$  invariant-mass range. For simplicity, the same model is used for the two experiments. However, the fitted model differs slightly from that used to generate events in order to account for the lack of knowledge of the underlying physics. The invariant mass of the signal is modelled by the sum of a Crystal Ball function, describing the core distribution, and a Gaussian describing the tails. Backgrounds are modelled by the same functional forms used to generate events. The signal peak position and all the combinatorial background parameters are varied in the fit, as well as the yields of the three events species. All the other parameters are fixed. The PDFs used in the fits are summarised in Tab. 2.

Table 2: Summary of the model used to fit events. Parameter notations are the same as in Tab. 1. Values of fixed parameters are given in the “Value” column; “Gen.” means that the fixed value is identical to that used for generation. The parameters  $\mu^{\text{tail}}$  and  $\mu_{\text{CB}}^{\text{core}}$  are constrained to take the same value.

Event species	Function	Parameter	Value
Signal	Sum of a core CB function and a Gaussian tail	$N$	varied
		$\mu_{\text{CB}}^{\text{core}}$	varied
		$\sigma_{\text{CB}}^{\text{core}}$	$1.5 \text{ GeV}/c^2$
		$\alpha^{\text{core}}, n^{\text{core}}$	Gen.
		Fraction of tail	Gen.
		$\mu^{\text{tail}}$ $\sigma^{\text{tail}}$	$= \mu_{\text{CB}}^{\text{core}}$ $3.8 \text{ GeV}/c^2$
Peaking background	Gaussian	$N$	varied
		$\mu$	$122 \text{ GeV}/c^2$
		$\sigma$	$5 \text{ GeV}/c^2$
Combinatorial background	4 <sup>th</sup> order Chebyshev polynomial	$N$	varied
		$c_1, c_2, c_3, c_4$	varied

After fitting each of the individual samples, we obtain combined results for the mass of the resonance and the branching fraction by two different methods:

1. a naïve average of the individual results, taking into account the parabolic errors of the fits to the individual samples;
2. a joint fit to the two samples in the **JFIT** framework, following the method proposed in this paper, using the full likelihood function.

As the likelihood functions are fairly Gaussian, asymmetric uncertainties have not been considered for the naïve averaging. The typical statistical uncertainty obtained by the two methods is 0.0027 for the branching fraction and  $0.054 \text{ GeV}/c^2$  for the mass of the resonance. Moreover, no bias has been observed in the extraction of the mass of the resonance by the two methods, while they both show a negative bias in the extraction of the branching fraction, as expected from the differences between generation and fit models. The results of the two methods for the resonance

branching fraction are compared in Fig. 2. In this particular case, the bias induced by the two methods is similar and thus the central values are in a good agreement. There is a small effect on the statistical uncertainty, which is very slightly overestimated in naïve averages. This behaviour may differ, in size and direction, in other cases. For instance, the statistical error on the mass of the resonance was, conversely, found to be underestimated in naïve averages. However, as the joint fits correctly take into account all correlations, they provide more reliable results.

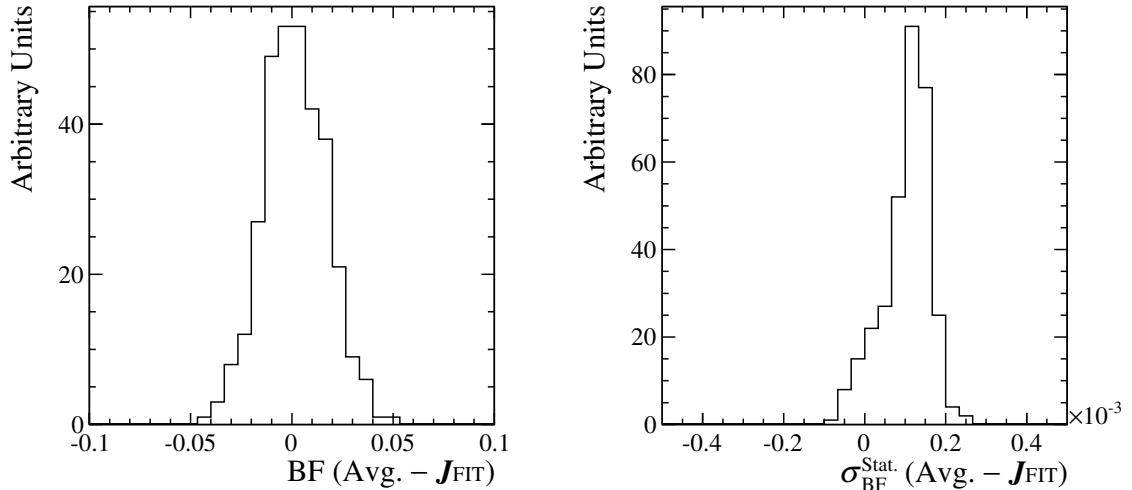


Figure 2: The distribution of the difference between the results of combinations performed by naïve averaging and  $\mathbf{JFIT}$ , for the (left) central values of the resonance branching fraction, and the (right) corresponding statistical uncertainties. The former shows that there is no difference in the bias induced by the two methods, and the latter shows that the statistical uncertainty is overestimated by 5% in naïve averages.

We expect larger differences between the two combination methods to arise when systematic uncertainties are evaluated. Parameters of the peaking background are considered to be badly known and, as such, to be sources of systematic uncertainties. To evaluate the effect from the width of the distribution, the corresponding PDF parameter is fixed to values  $2 \text{ GeV}/c^2$  above and below its nominal value, namely  $3.0 \text{ GeV}/c^2$  and  $7.0 \text{ GeV}/c^2$ . The variations of the resulting resonance mass and branching fraction are considered as systematic uncertainties. The same procedure is applied in individual and joint fits. Figure 3 shows a comparison between the systematic uncertainties obtained in naïve averages, where the individual systematic effects are considered to be 100% correlated, and in  $\mathbf{JFIT}$ s. Differences are due to the fact that correlations are correctly taken into account in joint fitting. The comparison shows clearly that the effect on systematic uncertainties can be large (in some cases more than twice the statistical uncertainty or 10% of the systematic uncertainty), and they may be either underestimated or overestimated by averaging the results.



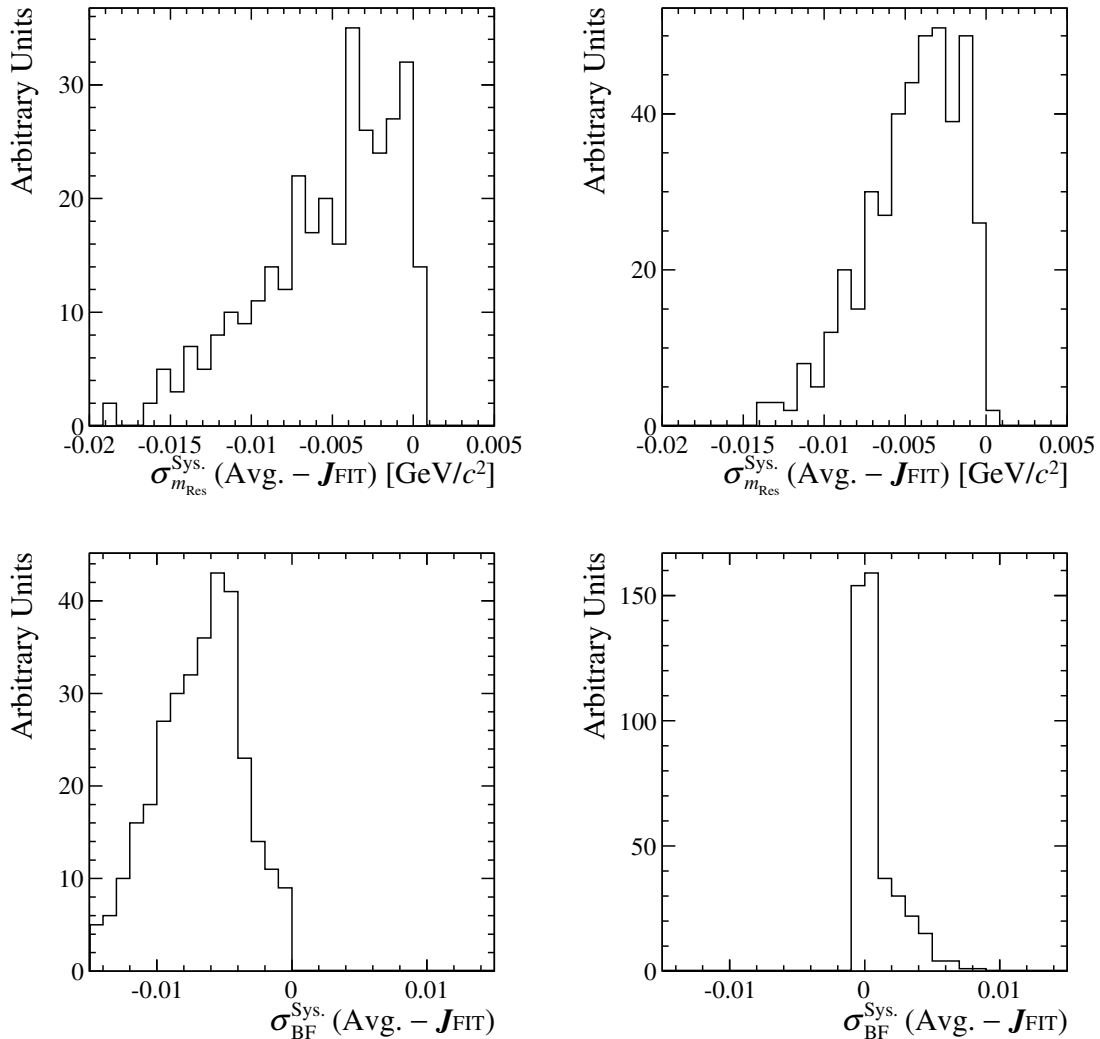


Figure 3: The difference between the systematic uncertainty values obtained in naïve averages and in  $\mathbf{JFIT}$ s. The systematic uncertainty considered is that arising from the width of the peaking background component. The naïve averages assume that the systematic effects are 100% correlated between the two experiments. The effect on both (top)  $m_{\text{Res}}$  and (bottom) the branching fraction, is shown for a peaking background Gaussian width of (left)  $3.0 \text{ GeV}/c^2$  and (right)  $7.0 \text{ GeV}/c^2$ . In most of the cases the uncertainty is underestimated by naïve averaging. The exception is the uncertainty on the branching fraction obtained by increasing the width to  $7.0 \text{ GeV}/c^2$  (bottom right plot).

## 4.2 Amplitude analysis of a three-body $B$ -meson decay

A second example is from the domain of flavour physics. It involves a larger number of parameters in the fit, and illustrates other advantages of the  $\mathbf{JFIT}$  method. For simplicity, we consider signal events only.

A key part of the physics programme of the  $B$ -factories, *BABAR* and *Belle*, consisted of amplitude (Dalitz-plot) analyses of 3-body  $B$ -meson decays [9]. More

recently such studies are performed by the LHCb experiment (see, for example, Refs. [10, 11]), and, in the near future, will be also undertaken by Belle-II. These analyses provide measurements of CKM angles and access to observables sensitive to new physics as well as information on the resonant structure of decays. At the same time, such analyses have a strong dependence on model assumptions. In general, these analyses are limited by the sample size and therefore working with a larger, common dataset could be a fruitful approach. Besides the benefit of grouping the expertise of the different collaborations, a joint analysis has many advantages compared to a simple combination of results from separate analyses. Firstly, a joint analysis provides a more powerful determination of which components should be in the signal model, and allows setting better limits on minor components. It is important to notice that minor, poorly determined signal components are a major source of the so called model uncertainty that is often a large systematic effect in Dalitz-plot analyses. Secondly, the fact that different collaborations often use different parameterisations of resonant decay modes in the signal model (e.g., resonance lineshapes and phase conventions) can lead to difficulties in comparing their results. In some cases a direct comparison of such results can be less meaningful; they are less useful for the community, and averaging them becomes non trivial. The coordination of signal models, which is a *sine qua non* for a joint fit, is therefore beneficial. These two advantages of joint fits are not explicitly illustrated in this work.

To exemplify direct advantages of the **JFIT** method, we use the result of the *BABAR* Dalitz-plot analysis of  $B^\pm \rightarrow K^\pm \pi^\mp \pi^\pm$  decays [12]. This analysis provided  $CP$ -averaged branching fractions and direct  $CP$  asymmetries for intermediate resonant and non-resonant contributions. It reported evidence for direct  $CP$  violation in the decay  $B^\pm \rightarrow \rho^0(770)K^\pm$ , with a  $CP$ -violation parameter  $A_{CP} = (44 \pm 10 \pm 4^{+5}_{-13})\%$ , where the first quoted uncertainty is statistical, the second is systematic, and the third is the model uncertainty mentioned above. The Belle collaboration also reported evidence of direct  $CP$  violation in the same decay mode [13] with a similar significance. This gives a strong motivation to obtain a combined result.

In the *BABAR* analysis, the contributions of the different intermediate states in the decay were obtained from a maximum-likelihood fit of the distribution of events in the Dalitz plot formed from the two variables  $m_{K\pi}^2 \equiv m_{K^\pm \pi^\mp}^2$  and  $m_{\pi\pi}^2 \equiv m_{\pi^\pm \pi^\mp}^2$ . As in many other Dalitz-plot analyses, the total signal amplitudes  $A$  and  $\bar{A}$  for  $B^+$  and  $B^-$  decays, respectively, were given in the isobar formalism, by

$$A = A(m_{K\pi}^2, m_{\pi\pi}^2) = \sum_j c_j F_j(m_{K\pi}^2, m_{\pi\pi}^2) \quad (5)$$

$$\bar{A} = \bar{A}(m_{K\pi}^2, m_{\pi\pi}^2) = \sum_j \bar{c}_j \bar{F}_j(m_{K\pi}^2, m_{\pi\pi}^2), \quad (6)$$

where  $j$  is a given intermediate decay mode. The distributions  $F_j \equiv \bar{F}_j$  are the lineshapes (e.g., Breit–Wigner functions) describing the dynamics of the decay amplitudes, and the complex coefficients  $c_j$  and  $\bar{c}_j$  contain all the weak-phase dependence and are measured relative to one of the contributing channels. They were

parameterised as

$$\begin{aligned} c_j &= (x_j + \Delta x_j) + i(y_j + \Delta y_j) \\ \bar{c}_j &= (x_j - \Delta x_j) + i(y_j - \Delta y_j), \end{aligned} \tag{7}$$

where  $\Delta x_j$  and  $\Delta y_j$  are  $CP$ -violating parameters.

We generate 100 signal-only datasets from the results of this analysis. The sample size is Poisson-distributed with an expected value of 4585, which is the signal yield obtained in the fit to the *BABAR* data [12]. We then consider each of the 4950 possible pairwise combinations of these samples as datasets from two different experiments. For the purpose of this example we focus on one of the parameters of interest of the *BABAR* analysis: the  $CP$  violating parameter  $\Delta x$  of the  $\rho^0(770)K^\pm$  contribution,  $\Delta x_\rho$ . The value used to generate events is the one measured by *BABAR*, namely  $-0.160 \pm 0.049 \pm 0.024^{+0.094}_{-0.013}$ . After fitting each of the individual samples with the model used for event generation, we obtain combined results for  $\Delta x_\rho$  by three different methods:

1. a naïve average of the individual results for  $\Delta x_\rho$ , taking into account the parabolic errors of the fits to the individual samples;
2. a naïve average, taking into account the asymmetric errors of the individual fits<sup>2</sup>, following the prescription from Ref. [1];
3. a joint fit to the two samples in the **JFIT** framework, following the method proposed in this paper, using the full likelihood function.

The results obtained from methods 1 and 2 above are found to be equivalent: in the present case, with a very few exceptions, the effect of the asymmetric nature of the likelihood is negligible comparing to the statistical uncertainty. The results obtained from methods 2 and 3 are compared in Fig. 4, and show a much larger difference. The distribution of the difference between results obtained by the two methods has a full width at half maximum of approximately 10% of the typical statistical uncertainty on  $\Delta x_\rho$  in fits to individual datasets (which is 0.03).

We perform likelihood scans as a function of  $\Delta x_\rho$  for several individual datasets and their corresponding joint fits, i.e., we fix  $\Delta x_\rho$  to several consecutive values, for each of which the fit is repeated. The other parameters are free to vary as in the nominal fit. We compare the sum of likelihood functions obtained in this way from two datasets to the likelihood scan obtained with the corresponding **JFIT**; this is shown in Fig. 5. This comparison illustrates the fact that even if two experiments provide their full likelihood dependences on certain parameters, obtaining a combined result by summing up these functions is not equivalent to performing a joint fit. Indeed, values of nuisance parameters, for which combined results are not desired, generally differ between the joint fit and the individual fits. Note that in the particular case shown in Fig. 5 the minimum obtained from the joint fit is closer to the generated value of  $-0.16$  and has a smaller error than the other combination. Also, the joint-fit result is smaller than both minima obtained from the individual

---

<sup>2</sup> The asymmetric error are obtained from the MINOS routine of the MINUIT package.

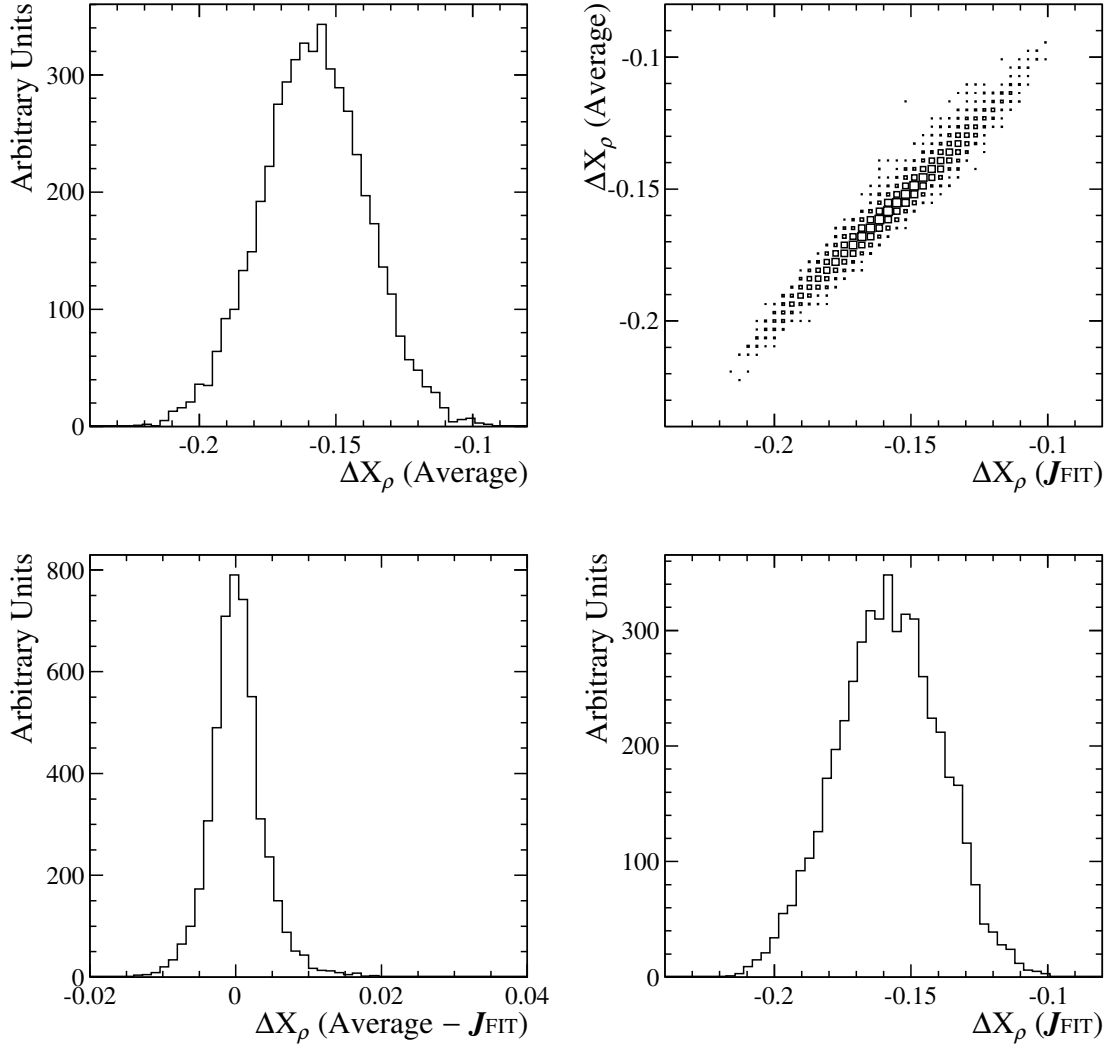


Figure 4: Distributions of  $\Delta x_\rho$  results obtained by (top left) naïve averages taking into account the asymmetric errors of the individual fits to two samples, (bottom right)  $J_{FIT}$ s (top right) the former versus the latter and (bottom left) the difference between the two.

fits. This indicates that even in well-behaved cases and even if the combination is performed by summing likelihood functions, neglecting correlations may result in biases.

To evaluate potential bias induced by naïve averaging, the distance of combined results to the generated value was compared between naïve averages, taking into account the asymmetric error, and  $J_{FIT}$ s. This study shows that results obtained by joint fits are more often closer to the generated value than those obtained by naïve averages due to the fact that they fully account for the correlations between the fit variables. Figure 6 shows the distance-from-generated-value of  $\Delta x_\rho$  results obtained by naïve averaging versus the corresponding quantity for  $J_{FIT}$ s, and the distribution of the difference between the former and the latter. To clarify the presence of the non-Gaussian tails in this distribution, it is overlaid with a Gaussian fitted to its central

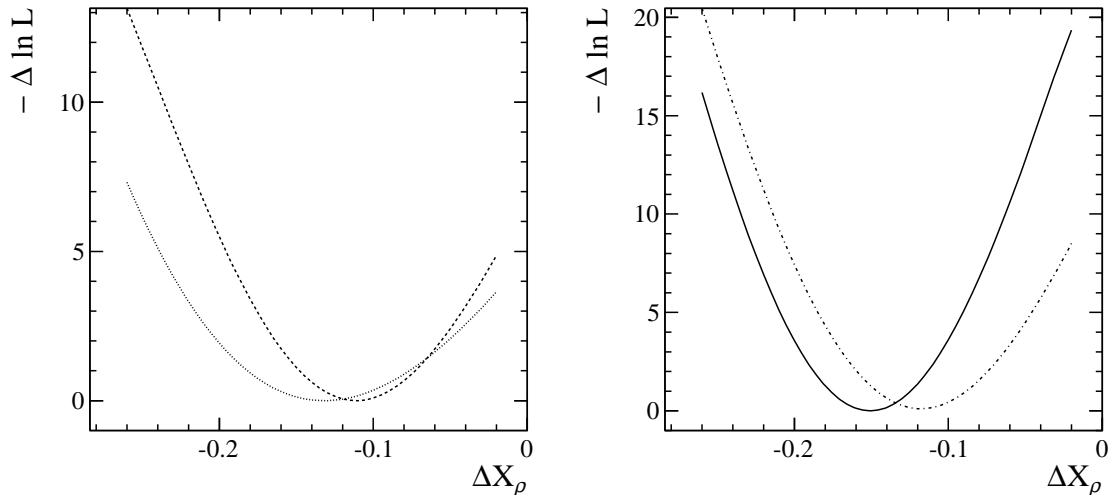


Figure 5: Left: Likelihood scans, showing  $-\Delta \ln \mathcal{L} \equiv (\ln \mathcal{L})_{\min} - \ln \mathcal{L}$  as a function of  $\Delta x_\rho$  in two different datasets. Right: the sum of these likelihoods (dashed-dotted curve), compared to the likelihood obtained from a **JFIT** to the two samples (solid curve). It should be noted that the result obtained from the joint fit is smaller than both of those from the individual fits and is closer to the true value ( $-0.16$ ). In addition it has a smaller uncertainty than the simple average.

region  $[-0.005, 0.005]$ ; numbers of positive and negative entries in the distribution, excluding the ranges corresponding to one, two and three standard deviations of the Gaussian are given in Table 3. Comparison of the statistical uncertainties obtained from naïve averages and **JFITS** are shown in Fig. 7. In 88% of the cases the error obtained from a joint fit is smaller.

Table 3: The distribution on the right hand side of Fig. 6 illustrates the fact that results obtained by joint fits are more often closer to the generated value than these obtained by naïve averages. Here are given the numbers of positive and negative entries in the distribution, excluding the ranges corresponding to one, two and three standard deviations ( $\sigma$ ) of the overlaid Gaussian.

Excluded region ( $\sigma$ )	Number of positive entries	Number of negative entries
3	126	71
2	330	266
1	918	911

We stress that the example given here is not extreme: likelihoods are nearly Gaussian and are rather well behaved, as can be seen in Fig. 5. In cases where the likelihood presents strong non-linear features, such as asymmetric functions that cannot be well described by a bifurcated Gaussian, or if it has multiple minima, the difference between naïve averaging and joint fitting could be much larger. In practice, multiple solutions appear in nearly all the Dalitz-plot analyses performed by the *B* factories; they represent one of the major difficulties in these analyses.

Clearly, a joint fit allows to resolve better the global minimum from the mirror solutions.

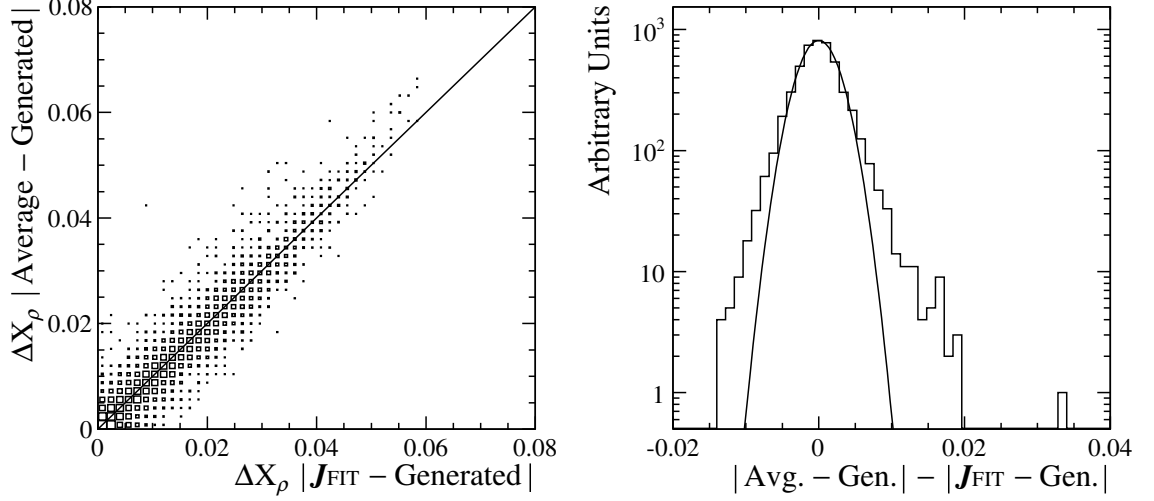


Figure 6: Left: distance from the generated value ( $-0.16$ ) of  $\Delta x_\rho$  results obtained by naïve averaging versus that corresponding to  $\mathbf{J}$ FITs. Right: distribution of the difference between the former and the latter. The solid smooth curve is a Gaussian fitted to the central region of the distribution  $[-0.005, 0.005]$ , to clarify the presence of the non-Gaussian tails.

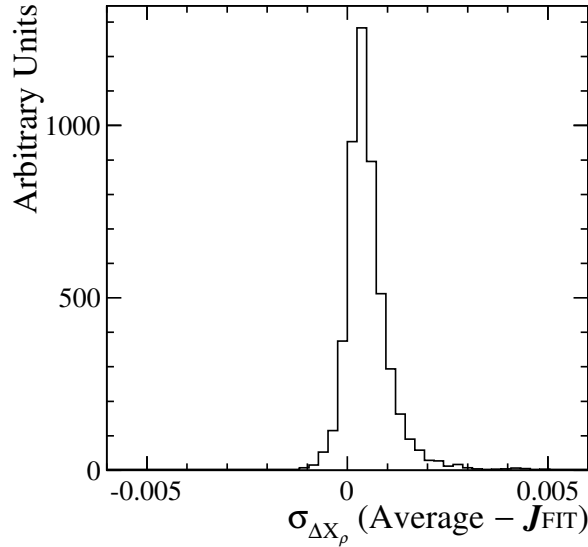


Figure 7: The difference between errors obtained in naïve averages, and those from  $\mathbf{J}$ FITs. In the former, the average between the positive and negative asymmetric errors is used. In 88% of the cases joint fits yield improved sensitivity to  $\Delta x_\rho$ .

## 5 Conclusions

In this paper, we have presented **JFIT**: a framework for obtaining combined experimental results through joint fits of datasets from several experiments. Using a master-server architecture, the tool allows such fits to be performed keeping the data separated and using independent fitting frameworks, thus simplifying the process with respect to data access policies. It also allows to save resources: the analysis framework of each experiment can be readily reused and there is no need to write the data in a common format. The tool is implemented in the Laura++ package [5], using the network communication classes from the ROOT framework (TMessage, TMonitor, TServerSocket and TSocket).

The usefulness of the approach has been illustrated by two examples: one from the domain of resonance searches, and the other from amplitude analyses in flavour physics. Correctly accounting for correlations between parameters in likelihood functions in different experiments, which is an intrinsic property of joint fits, results in improved results, and more reliable uncertainties. Thus, these fits provide a means to better exploit data from multiple experiments.

## Acknowledgments

The work presented in this paper was started in the purpose of performing joint analyses between the *BABAR* and Belle collaborations. During his mandate as the *BABAR* spokesperson, François Le Diberder initiated this project and generated interest in it among the *BABAR* collaboration, the Belle management and collaboration, and the authors of ROOT. We would like to thank him for these actions and for fruitful discussions concerning this paper. We would also like to thank Roger Barlow for his extremely valuable advice and comments regarding the statistical aspects and examples. This work is supported by the Science and Technology Facilities Council (United Kingdom) and the European Research Council under FP7.

## References

- [1] J. Beringer *et al.* [Particle Data Group Collaboration], Phys. Rev. D **86**, 010001 (2012).
- [2] The web page of RooFit package: <http://roofit.sourceforge.net>
- [3] The web page of ROOT project: <http://root.cern.ch>
- [4] F. James, 1972 MINUIT - Function Minimization and Error Analysis CERN Program Library Long Writeup D506.
- [5] The development page for the Laura++ project: <http://laura.hepforge.org>
- [6] M.J. Oreglia, Ph.D Thesis, SLAC-236(1980), Appendix D; J.E. Gaiser, Ph.D Thesis, SLAC-255(1982), Appendix F; T. Skwarnicki, Ph.D Thesis, DESY F31-86-02(1986), Appendix E.
- [7] G. Aad *et al.* (ATLAS Collaboration), Phys. Lett. B **716**, 1 (2012).
- [8] S. Chatrchyan *et al.* (CMS Collaboration), Phys. Lett. B **716**, 30 (2012).
- [9] A. J. Bevan *et al.* (BABAR and Belle Collaborations), arXiv:1406.6311 [hep-ex].
- [10] R. Aaij *et al.* (LHCb Collaboration), Phys. Rev. D **87**, 072004 (2013).
- [11] R. Aaij *et al.* (LHCb Collaboration), arXiv:1407.7712 [hep-ex]. To appear in Phys. Rev. D.
- [12] B. Aubert *et al.* (BABAR Collaboration), Phys. Rev. D **78**, 012004 (2008).
- [13] A. Garmash *et al.* (Belle Collaboration), Phys. Rev. Lett. **96**, 251803 (2006).